

# Energy Distribution and Redistribution and Chemical Reactivity. The Generalized Delta Overlap-Density Method for Ground State and Electron Transfer Reactions: A New Quantitative Counterpart of Electron-Pushing<sup>1</sup>

Howard E. Zimmerman\* and Igor V. Alabugin<sup>‡</sup>

Contribution from the Department of Chemistry, University of Wisconsin–Madison, Madison, Wisconsin 53706

Received July 3, 2000. Revised Manuscript Received January 4, 2001

**Abstract:** A new approach to prediction of organic reactions and understanding of the electron flow involved in the reaction mechanisms is presented. The method developed permits comparison of electronic structures of species different in multiplicity, charge, and geometry based on use of spin- and charge-independent entities—“overlap corrected density matrices”. The method utilizes the basis orbitals of one molecule A (e.g. reactant) in the computation of a second molecule, B, derived from the first by an approach to product. This then provides two Overlap-Density Matrices with a common set of basis (e.g. hybrid) orbitals. Subtraction of Overlap-Density Matrix B from Matrix A affords the Delta Overlap-Density Matrix. Each element of the Delta Overlap-Density matrix gives the change in electron population of a bond or of a single hybrid orbital. Molecule B may differ from A by the addition or loss of an electron, by stretching of a bond, by electronic excitation, or by some other perturbation. The Delta Overlap-Density matrices afford a detailed description of the reaction process and provide predictions of overall reactions including such subtleties as regiochemistry.

## Introduction

A major endeavor in organic chemistry is the development of quantitative methodology parallel to the remarkable power of “electron pushing”. The presently described research takes a new tact, one that is capable of providing a quantitative prediction of molecular reactivity. This involves comparison of the reacting species, on its way to product, with the reactant itself. For this, several items were required. First, we needed a set of orbitals common to reactant and to the partially reacted species. Second, we wanted these orbitals to be a localized set of a type used in organic mechanistic reasoning. Third, we required a method of comparison of the two species in terms of these localized orbitals.

## An Outline of the Method

Recently<sup>2</sup> we described the use of Delta Density matrices for predicting photochemical reactions. The method compared excited state with ground-state density matrices,<sup>3</sup> both having ground state geometry. Presently we extend the concept to permit comparison of molecular pairs more generally. While a spin-averaged (e.g. CASSCF) density matrix for a molecule certainly will depend on the singlet, doublet, or triplet multiplic-

ity, the density matrix, once obtained, no longer contains spin or number of electrons explicitly. This means that the spin-averaged density matrix merely characterizes chemical bonding and electron densities of each species. Hence it is acceptable to compare density matrices of different states of a molecule. Furthermore, it is also acceptable to compare the density matrix of a given molecule and that of the molecule deformed, perhaps reacting toward product.

However, it is a requirement that both species, whose density matrices are to be compared, have their wave functions expressed in terms of the same basis set of localized orbitals. A most convenient set of localized orbitals is the Weinhold natural hybrid orbitals (i.e. the NHO's).<sup>4</sup> We have used the NHO's as our basis both in our previous study<sup>2</sup> and in the present investigation. The NHO's look like the organic chemist's version of hybrids, two constituting a  $\sigma$  bond and being directed at one another; lone pair hybrids as well as  $\pi$ -system p-orbitals are also used in the NHO set. Importantly, the NHO hybrids constitute an untruncated orthogonal set. Now, to use the same basis set of NHO's, we utilize the hybrid orbitals of the initial molecule, generally the reactant as a reference point. This is accomplished by extracting the set of NHO's of the reactant and requiring the second species to be defined in terms of this set. Thus the hybrid orbitals of one molecular species (e.g. the reactant) are written out and used in obtaining its density matrix. Then we read these same basis orbitals in for use in computation of the density matrix of the second molecular species. The main limitation is that the two species being compared cannot differ dramatically in geometry.

<sup>‡</sup> Current address: Department of Chemistry, Florida State University, Tallahassee, FL 32306.

(1) (a) This is Paper 258 of our general series. (b) For Paper 257 see: Zimmerman, H. E.; Lapin, Y. A.; Nesterov, E. E.; Sereda, G. A. *J. Org. Chem.* **2000**, *65*, 7740–7746.

(2) Zimmerman, H. E.; Alabugin, I. V. *J. Am. Chem. Soc.* **2000**, *122*, 952–953.

(3) Also in that publication we included overlap as a factor in the density matrices. However, considering that the off-diagonal elements between two orbitals are modified by this extent of overlap, we now term these as “Overlap-Density” elements.

(4) (a) Foster, J. P.; Weinhold, F. *J. Am. Chem. Soc.* **1980**, *102*, 7211–7218. (b) Reed, A.; Curtiss, L. A.; Weinhold, F. *Chem. Rev.* **1988**, *88*, 899–926. (c) Weinhold, F. In *Encyclopedia of Computational Chemistry*; Schleyer R. V. R., Ed.; Wiley: New York, 1998; Vol. 3, p 1792.

The method permits us to monitor the flow of electron density in single orbitals and in bonds as reactions proceed. We then can follow ground-state reactions, electron-transfer processes, as well as photochemical transformations. We term this extended method the Generalized Delta Overlap-Density method.

Our Delta Overlap-Density matrix elements are defined as in eq 1 with superscript "a" referring to a reactant species and "b" referring to the second molecule. In dealing with reactions, superscript "a" refers to the reactant while "b" refers to a species further along the reaction coordinate, possibly on the same hypersurface. Or, species "b" may be a radical anion, radical cation, or excited state. The subscripts "r" and "t" refer to the two hybrid or p orbitals; here we use Weinhold NHO's. The  $S_{rt}$  terms are overlap integrals to take into account the relative signs

$$\Delta D_{rt} = D_{rt}^b S_{rt}^b - D_{rt}^a S_{rt}^a \quad (1)$$

of these hybrid basis orbitals and also distances between orbital pairs. The hybridization as well as orientation of corresponding NHO's may, in fact, vary during reaction but we are probing only electron densities. The corresponding NHO pairs—reactant and second reacting species—are correlated by use of the reactant NHO's as a common basis.

Thus as a molecule is transformed from species A to B, each diagonal element  $\Delta D_{rt}$  (i.e.  $r = t$ ) gives the change in electron density in a hybrid orbital while each off-diagonal element gives the change in electron density between hybrids  $r$  and  $t$ . These  $\Delta D$  elements are really just changes in bond order or one-center density in the process of proceeding from A to B. Three cases may be considered. (i) A and B may be ground and excited states, respectively. (ii) B may derive from A by gain or loss of one electron as in radical anion or radical cation formation. (iii) B may result from perturbation of one or more bonds of A. In the first two instances, there is the common geometry of A that is employed, while in the last instance the molecular geometry is perturbed from that of A. Hence a variety of transformations are subject to our analysis.<sup>5</sup>

The generalized Delta Density-Overlap method provides a quantitative counterpart of chemical intuition. Also, it is highly flexible in that it can be applied to virtually any electronic state of interest by using any quantum mechanical approach capable of affording density matrices. The NBO analysis permits description of the wave function in terms of localized hybrid orbitals (NHO's) as a basis and thus is closely related to chemical bonding concepts.

## General Results

Presently we describe eight examples of the Generalized Delta Density Method as typical: (a) the cyclopropyl ketone three-ring opening on one-electron introduction and its regioselectivity, (b) the reaction of the radical cation of a benzylsilane, (c) the regiochemistry of the ring opening of the methoxy-bicyclohexane radical-cation, (d) the solvolysis of dehydronorbornyl chloride, (e) the quenching of an  $n-\pi^*$  ketone singlet by amines, (f) the extent of electron transfer in  $n-\pi^*$  hydrogen abstraction, (g) the Birch reduction, and (h) the  $S_N2$  process.

In each example the Delta Overlap-Density treatment leads to predictions of the reaction course and also permits one to follow the flow of electron density during the reaction. Electron density changes are obtained for every bond and every non-bonding orbital of the species as it reacts. Thus we obtain

(5) Our Communication in ref 2 describes some examples of vertical (i.e. Franck-Condon) excitations where negative  $\Delta D$  elements permit prediction of which bonds have become weakened.

detailed information about which bonds are weakened or forming and how the electron density is redistributed.

The density matrices in the NBO basis were obtained using CASSCF computations. The NBO 4.0 program was used as interfaced to the GAUSSIAN 98.<sup>6</sup> Each  $\Delta D$  element results from double products— $S_{rt}$  and  $D_{rt}$ —each one of which is less than unity. Thus, the  $\Delta D$  values are scaled by 10 000 for convenience. In this context, we note that transfer of 0.001 electron corresponds approximately to 1 kcal/mol. Thus a value of 10 after scaling is chemically significant. Finally the geometries employed are depicted in Scheme 1.

## Choice of Active Space and Basis Orbitals

CASSCF was employed throughout. The active space utilized was determined by increasing this until no appreciable differences in computational results were observed. Molecular orbitals of appropriate symmetry were selected using the option Guess = Alter in Gaussian98. Then, commonly, a still larger space was employed where computationally practical. In the case of the choice of starting basis orbitals, both 3-21G\* and 6-31G\* sets were used. The differences generally proved minor and the choice depended on computational practicality. Reactant structures were generated with HF/6-31G\* or CASSCF geometry optimization and a 6-31G\* basis. However, it should be recognized that the Delta Overlap-Density method affords results for whatever structures are employed and is relatively insensitive to slight variations in structure. Thus even semiempirical structures could, in principle, be employed and be of interest.

## Use of an NHO Basis: The Nature of NHO Hybrid Orbitals and Their Relation to Pre-NHO Hybrids

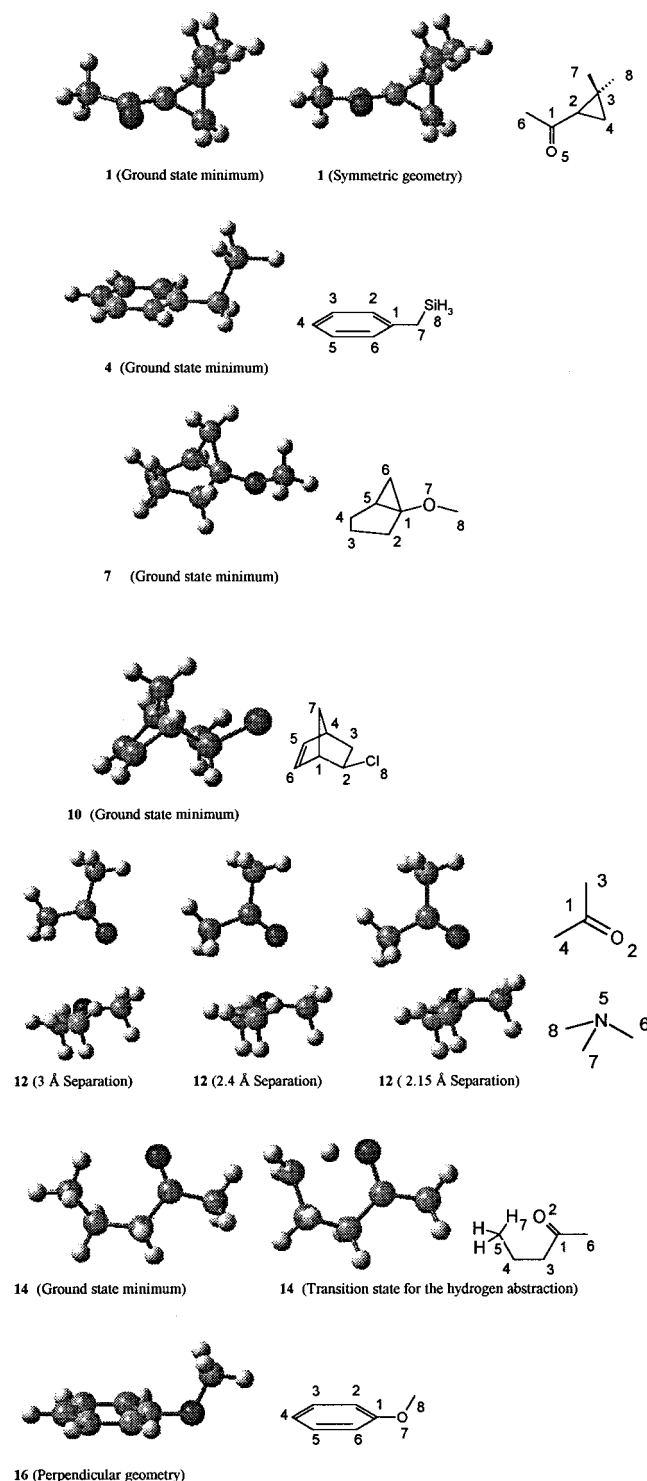
The basis used was the Weinhold NHO set. Unlike the Pre-NHO hybrids, the NHO set is orthogonalized. In the Weinhold treatment, this results in minor "tails" with reversed sign, which accomplish the orthogonality. These tails tend to accumulate in the core of adjacent atoms and in any event NHO's with tails do give proper bond energies. To establish a common basis, one uses an NAONBO conversion (e.g.  $\text{naonbo} = w$ ). The output is written in the basis of the original computation including the eigenvectors and density matrix in an NHO basis. For a second molecule of interest, by using the same conversion, but reading in (e.g.  $\text{naonbo} = r$ ) the basis, one then obtains results in the NHO basis stored from first computation.

Finally, our use of NHO density matrix elements multiplied by Overlap Matrix Elements has several functions. This takes care of basis set relative sign problems. Also, it includes a distance function so that a more meaningful bond order results.

## Utility of the Density Matrix for Comparison of Different States and Species

The Density Matrices are spin-free entities. From CASSCF computations they are one-electron density matrices. For triplet and odd-electron species, although  $\alpha$  and  $\beta$  spin density matrices

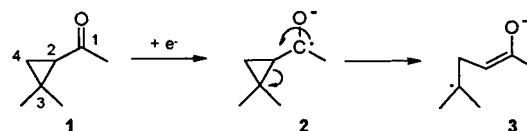
(6) Gaussian 98, Revision A.6, Frisch, M. J.; Trucks, G. W.; Schlegel, H. B.; Scuseria, G. E.; Robb, M. A.; Cheeseman, J. R.; Zakrzewski, V. G.; Montgomery, J. A., Jr.; Stratmann, R. E.; Burant, J. C.; Millam, J. M.; Daniels, A. D.; Kudin, K. N.; Strain, M. C.; Farkas, O.; Tomasi, J.; Barone, V.; Cossi, M.; Cammi, R.; Mennucci, B.; Pomelli, C.; Adamo, C.; Clifford, C.; Ochterski, J.; Petersson, G. A.; Ayala, P. Y.; Cui, Q.; K. Morokuma, K.; Malick, D. K.; Rabuck, A. D.; Raghavachari, K.; Foresman, J. B.; Cioslowski, J.; Ortiz, J. V.; Stefanov, B. B.; Liu, G.; Liashenko, A.; Piskorz, P.; Komaromi, I.; Gomperts, R.; Martin, R. L.; Fox, D. J.; Keith, T.; Al-Laham, M. A.; Peng, C. Y.; Nanayakkara, A.; Gonzalez, C.; Challacombe, M.; Gill, P. M. W.; Johnson, B.; Chen, W.; Wong, M. W.; Andres, J. L.; Gonzalez, C.; Head-Gordon, M.; Replogle, E. S.; Pople, J. A. Gaussian, Inc.: Pittsburgh, PA, 1998.

**Scheme 1.** Optimized Geometries for the Reagents in This Study

are available, it is the spin averaged matrices which are most valuable for the present purposes. The elements correlate nicely with bond orders and one-center electron densities.

### Specific Applications

The first case considered is the reaction of cyclopropyl ketone radical anions. These are known to undergo fission of the  $\alpha,\beta$ -bond of the three-membered ring. In the case of unsymmetrically substituted three-rings, it is the more alkylated bond that is cleaved (note Scheme 2). This is a result that would not have been a priori predicted.

**Scheme 2.** Three-Membered Ring Opening by Single Electron Introduction**Table 1.** Delta Density Values for the Cyclopropyl Radical Anion Formation<sup>a</sup>

entry	bonds	$\Delta D$	entry	one-center hybrid orbitals	$\Delta D$
1	C2-C4	-26	5	C(O)	+4989
2	C2-C3	-220	6	O(C)	+3071
3	C3-C4	-26	7	C2(C3)	-642
4	C=O	-1452	8	C3(C2)	+1106
			9	C2(C4)	-652
			10	C4(C2)	+1000
			11	C4(C3)	+39
			12	C3(C4)	-7

<sup>a</sup> CASSCF(8,8)/3-21G\* for the neutral molecule and CASSCF(9,8)/3-21G\* for the radical anion.

Alkylation of odd-electron centers is stabilizing while alkylation of carbanionic centers is destabilizing and, thus, the regioselectivity is a matter of odd-electron versus anionic control. Additionally, stereoelectronic effects result from conjugation of the carbonyl group with the three-ring depending on conformation. The experiment is known and it is of real interest to consider what theory predicts.<sup>7</sup>

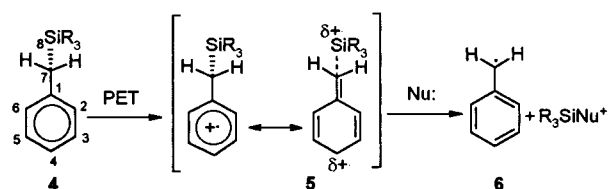
Delta Overlap-Density computational results for the geometry optimized cyclopropyl ketone on one-electron introduction revealed that it is the more substituted bond that has the more negative delta density value (note Table 1, entry 2 compared with entry 1). Still, the phenomenon is a bit more complicated since the geometry-optimized conformation is one with the carbonyl  $\pi$  system overlapping better with the dimethyl substituted three-ring bond than with the unsubstituted one. Thus it was of interest to obtain a delta density matrix from the conformation with the carbonyl group having the same favorable dihedral angle with the unsubstituted three-ring bond. The delta density values now favored fission of the less substituted bond but with a smaller delta density value (-95). This is to be compared with the -220 value for the more substituted bond (cf. Table 1). With a symmetric dihedral, the more substituted bond was marginally favored (-60 vs -58).

Interestingly, the change in electron density at the dimethylated  $\beta$ -carbon compared with that at the unsubstituted  $\beta$ -carbon reveals that in reduction, it is at the more substituted carbon where the electron density increases more (note Table 1, entry 8 vs entry 10) corresponding to the new density entering the orbital. However, the change is small, and in any event it is the bond order change that corresponds to bond strengths.

As expected from the known<sup>8</sup> drift of electron density in the  $\pi^*$  orbital of carbonyl compounds toward the carbonyl carbon, the  $\Delta D$  value at the carbonyl carbon in this case is most positive (entry 5). The high electron density here and in the carbonyl group in general might lead one to anticipate anionic behavior and the reverse regioselectivity. However, that is not the case as is clear from both experiment and the Overlap-Density treatment.

(7) (a) Dauben, W. G.; Wolf, R. E. *J. Org. Chem.* **1970**, *85*, 374-379. (b) In this instance the authors did the computation first and then inspected the literature. Thus, as noted in the discussion, a skilled organic chemist can predict many reactions but not every one. The regioselectivity was the point of uncertainty here.

(8) (a) Buckingham, A. D.; Ramsay, D. A.; Tyrrell *Can. J. Phys.* **1970**, *48*, 1242-1253. (b) Freeman, D. E.; Klemperer, W. *J. Chem Phys.* **1964**, *40*, 604-605(L).

**Scheme 3.** Radical Cation Benzylic–Silyl Fission**Table 2.**  $\Delta D$  Treatment for the Radical Cation of Benzylsilane **4**

bonds	“vertical” <sup>a</sup> $\Delta D$ value	bond length (neutral), Å	bond length <sup>b</sup> (radical–cation), Å
$\pi$ C1–C2	–804	1.4031	1.4346
$\pi$ C2–C3	+577	1.3957	1.3532
$\pi$ C3–C4	–732	1.3968	1.4161
$\pi$ C1–C7	+405	1.5217	1.4581
$\sigma$ C7–Si8	–428	1.9009	1.9928

<sup>a</sup> For the geometry corresponding to the global energy minimum for the neutral molecule. <sup>b</sup> Optimized radical–cation geometry (CASSCF(7,8)/3-21G\*).

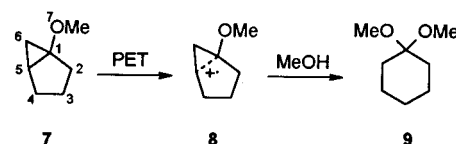
**Table 3.** One-Center  $\Delta D$  Values for the Radical Cation of Benzylsilane **4**

hybrid orbital	“vertical” one-centre $\Delta D$ value
C1( $\pi$ )	–2985
C2( $\pi$ )	–945
C3( $\pi$ )	–458
C4( $\pi$ )	–3175
C7(Si8)	+12
Si8(C7)	–589

Having dealt with a radical anion reaction, we proceeded to try the method on a radical cation example, that of the reaction of benzylsilane **4**. In this case, the radical cation is known<sup>9</sup> to undergo scission of the carbon to silicon bond as depicted in Scheme 3.

The Delta Overlap-Density treatment of the generation of the radical cation from the neutral species reveals the most negative off-diagonal element to correspond to the C–Si bond (note Table 2). Additionally, the  $\Delta D$  results exhibit an increase in several bond orders: ortho–meta and benzylic–ipso. The “vertical” (Franck–Condon) oxidation generates a “vibrationally hot” molecule and the  $\Delta D$  treatment affords predictions of molecular relaxation modes.<sup>10</sup> An increase in bond orders (i.e.  $\Delta D$  elements) suggests molecular relaxation by bond contraction while a decrease in bond orders predicts relaxation by bond lengthening. We see positive ortho–meta but negative ipso–ortho and meta–para  $\Delta D$  values which suggests bond contraction and bond lengthening, respectively. This, indeed, was seen in the bond lengths of the optimized radical cation (note Table 2, last column). Charge effects are given in Table 3.

Another example is that of the photochemical generation of the radical cation **8** as described by Gassman.<sup>11</sup> Experimentally, it is the internal three-ring bond that is broken (Scheme 4). In this case the regioselectivity is not a consequence of conformation since the C–O–C1–C5 dihedral is 149° while the C–O–C1–C6 dihedral is 78°, thus favoring oxygen p<sub>y</sub> orbital overlap with the out-of-plane bond. A Delta Overlap-Density computa-

**Scheme 4.** Radical Cation Regioselectivity of Bicyclic Ring Opening**Table 4.** Delta Density Values for the Radical Cation **8**

bond or orbital	CAS(5,6) <sup>a</sup>	CAS(7,7) <sup>b</sup>
C1–C5	–56	–1320
C1–C6	–594	–1008
C5–C6	–86	–152
C5(C1)	–676	–2205
C1(C5)	+538	–1379
C5(C6)	–308	–67
C6(C5)	+30	0
C1(C6)	+98	–1091
C6(C1)	–1824	–1906
O7(p, lone pair)	–6444	–234
O7(sp lone pair)	–156	–1134

<sup>a</sup> CASSCF(6,6)/3-21G\*//RHF/6-31G\* energy, –344.96684 au (S0); CASSCF(5,6)/3-21G\*, –344.69385 au (radical–cation). <sup>b</sup> CASSCF(7,7)/3-21G\*, –344.69481 au (radical–cation).

tion, performed with a CASSCF(7,7) for the radical cation **8** and (6,6) for the neutral reactant **7**, showed the weakest bond to be the internal one in accord with experiment.<sup>12</sup> Interestingly, with a smaller active space, it was the out-of-plane bond that was weakened most. The larger active space permitted electron removal from (HOMO-3), something that would not have been intuitively obvious and which frontier orbital reasoning would have missed. Inspection revealed that HOMO-3 is heavily weighted in the internal three-ring bond while (HOMO-1) and HOMO-2 weight this bond very little. Note Table 4. With a proper active space the Overlap-Delta Density analysis is in accord with the mechanism of Gassman based on the observed chemistry. Hence at least two conclusions are possible from these results. One is that the Delta Overlap-Density treatment predicts regiochemistry which is not a priori obvious. Second, the method reveals the potential pitfall of using too limited an active space and illustrates the risk in using frontier (e.g. HOMO-LUMO) molecular orbital reasoning.

The method proved equally useful in dealing with reactions other than electron transfer. Thus the method was applied to the solvolysis of dehydronorbornyl chloride. Here the two species used were the reactant and the partially ionized molecule. The C–Cl bond was stretched from 1.8 to 2.7 Å, but the geometry otherwise was unchanged. Not surprisingly, the C–Cl bond exhibited polarization with the chlorine picking up electron density and the carbon losing density. However, what is particularly interesting is the large depletion of electron density from the  $\sigma$ -bond between the bridgehead carbon and the double bond. As might be anticipated, there is also depletion from the  $\pi$ -bond. These effects are outlined pictorially in Scheme 5.

The results are reminiscent of the bond–bond polarizability analysis we presented earlier.<sup>13</sup> However, we note that here the interaction of the  $\sigma$ -bond in this case is larger than that of the  $\pi$ -bond in contrast to the polarizability results. However, the bond–bond polarizability computation involved a minor perturbation using only the reactant wave function while our Delta

(9) Baciocchi, E.; Massimo Bietti, M.; Lanzalunga O. *Acc. Chem. Res.* **2000**, *33*, 243–251.

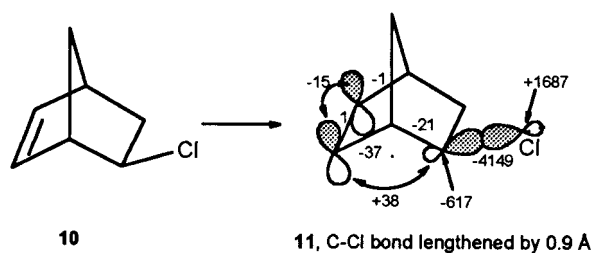
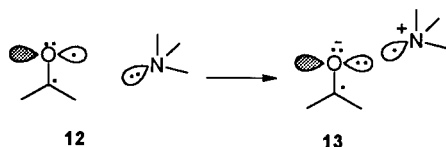
(10) (a) Zimmerman, H. E.; Gruenbaum, W. T.; Klun, R. T.; Steinmetz, M. G.; Welter, T. R. *J. Chem. Soc. Chem. Commun.* **1978**, 228–230. (b) For a recent example of the role of vibrational relaxation in photochemistry, see: Becker, R. S.; Pellicotti, A. P.; Romani, A.; Favaro, G. *J. Am. Chem. Soc.* **1999**, *121*, 2104–2109.

(11) Gassman, P. G.; Burns, S. J. *J. Org. Chem.* **1988**, *53*, 5576–5578.

(12) The other significantly weakened bond was the external cyclopropyl bond (–1008). It is possible that cleavage of this bond provided an alternative reaction pathway explaining moderate experimental yields in this reaction.

(13) Zimmerman, H. E.; Weinhold, F. *J. Am. Chem. Soc.* **1994**, *116*, 1579–1580.

## Scheme 5. Dehydronorbornyl Chloride Reaction

Scheme 6. Quenching of  $n-\pi^*$  Singlets by AminesTable 5. The  $\Delta D$  Analysis of PET between Acetone and Trimethylamine on the S1 Surface

distance, Å	$\Delta p_y(O)^a$	$\Delta n(N)^a$
2.4	+335	-576
2.15	+1408	-960

<sup>a</sup> The values are relative to  $D^a$ , the density matrix for excited acetone/trimethylamine system (S1) at 3 Å separation. The densities at this 3 Å reference point are 1.017 at the  $p_y$ -oxygen orbital and 1.912 at the lone pair of nitrogen (unscaled and original densities here).

Table 6.  $\Delta D$  Analysis of S0–S1 Excitation of the Acetone/Trimethylamine System at 3 Å Separation

distance, Å	$\Delta p_y(O)$	$\Delta n(N)$
3	-9005	-004

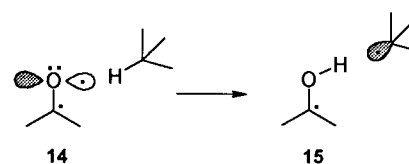
Overlap-Density treatment has considered electron density changes much further along the reaction coordinate (i.e. the bond stretching by 0.9 Å).

Another intriguing phenomenon is the quenching of carbonyl  $n-\pi^*$  singlets by amines<sup>14</sup> Note Scheme 6. We have employed the Delta Overlap-Density treatment to assess the extent of electron transfer as a function of the proximity of the ketone–amine pair. We do make the approximation here, as in the previous examples of electron transfer, that these “gas-phase” computations parallel the actual solution behavior at least qualitatively. Reference to Tables 5 and 6 shows electron transfer to become appreciable only at a 2.4 Å approach. Thus Table 5 shows that as the distance between the carbonyl oxygen and the amine nitrogen decreases from 3 Å to 2.4 Å and then to 2.15 Å the electron density at nitrogen decreases while that in the  $p_y$  orbital increases. However, we see that this effect is appreciable only at the shorter distance and that some orbital contact is needed.

Table 6 uses our original vertical excitation approach and we see that at 3 Å the  $p_y$  orbital has lost slightly less than one electron on  $n-\pi^*$  excitation (a value of 10 000 would correspond to loss of one electron). Some of this less than unity loss comes from the nitrogen and some derives from the acetone methyl to carbonyl carbon  $\sigma$ -bonds (i.e. hyperconjugative, and incipient Norrish I delocalization from  $C_1C_3$  and  $C_1C_4$  bonds, Scheme 1). In any case, the amount of donation from nitrogen at this 3 Å distance is seen to be minor.

Somewhat similar and of equal importance is the question of the intricate details of triplet  $n-\pi^*$  hydrogen abstraction.

(14) For references to amine quenching see: Yoon, U. C.; Mariano, P. S.; Givens, R. S.; Atwater, B. W., III In *Advances in Electron-Transfer Chemistry*; Mariano, P. S., Ed.; JAI Press: Greenwich, CT, 1994; Vol. 4, pp 53–116.

Scheme 7.  $n-\pi^*$  Hydrogen AbstractionTable 7.  $\Delta D$  Analysis of  $n-\pi^*$   $\gamma$ -Hydrogen Abstraction in 2-Butanone

	vertical (S0–T1) $\Delta D$ elements at S0 geometry <sup>a</sup>	TS (S0–T1) $\Delta D$ elements at T1 TS geometry <sup>b</sup>	T1 $\Delta D^c$ from vertical to TS
C–H	+24	-1539	-1553
H- $p_y(O)$	-1	+1173	+1174
$p_y(O)$	-7653	-3409	+4144
C(H)	-146	-4693	-4547
H(C)	+134	-101	-235

<sup>a</sup>  $\Delta D$  elements are for the S0–T1 vertical transition, ground-state geometry (2.5 Å O–H distance). <sup>b</sup>  $\Delta D$  elements for the S0–T1 vertical transition at T1 transition state geometry (1.19 Å O–H Distance). <sup>c</sup>  $\Delta D$  elements on T1 surface with the O–H distance decreasing from 2.5 to 1.19 Å. (i.e. vertical excitation vs transition state geometry).

Table 8.  $\Delta D$  and NBO Analysis of Electron Density Distribution for Radical–Anion 17

	$\Delta D$	total charge	$\pi$ density (radical–anion)
C1	+367	0.349	0.990
C2(o-trans)	+2849	-0.468	1.316
C3(m-trans)	+1090	-0.285	1.098
C4	+515	-0.275	1.096
C5(m-cis)	+3417	-0.444	1.316
C6(o-cis)	+1311	-0.406	1.210

Note Scheme 7. Table 7 utilizes values for  $\gamma$ -hydrogen abstraction in 2-butanone. One might question whether the process occurs by  $p_y$ -orbital attack on a hydrogen or, instead, by first transfer of a single electron from the C–H bond to the  $p_y$ -orbital, followed by proton transfer. In this case we used the QST3 option in Gaussian98 to locate the transition state (an O–H separation of 1.19 Å) and obtained  $\Delta D$  elements as a function of proximity of the  $p_y$ -orbital and the hydrogen atom. Table 7 contains two types of information. Data columns 1 and 2 of the table deal with  $\Delta D$  effects resulting from vertical (i.e. Franck–Condon) electronic excitation and ISC. Data column 3 deals with  $\Delta D$  effects resulting from motion on the triplet hypersurface. At the transition state on the triplet surface there was just partial electron transfer, i.e., 0.48 electron lost from the hybrid orbitals comprising the C–H bond with 0.41 electron going to the electron-deficient oxygen  $p_y$ -orbital (note entries 3, 4 and 5 of the last column of Table 7). With less than complete electron transfer at the transition state, we can conclude that the proton-transfer mechanism is not operating.

In the case of vertical excitation (data columns 1 and 2 of Table 7) we see the large negative increase in the  $\Delta D$  value for the C–H bond as the  $p_y$  orbital begins its approach. We also see the decreased electron deficiency of the oxygen  $p_y$  orbital as the carbonyl oxygen approaches the C–H hydrogen.

The Birch Reduction<sup>15</sup> is another case subject to Delta Overlap-Density analysis. Note Scheme 8 for the mechanism. In view of our interest in this reaction, we pursued the matter of electron density changes in the initial electron introduction just preceding the rate-limiting protonation. Here it is the

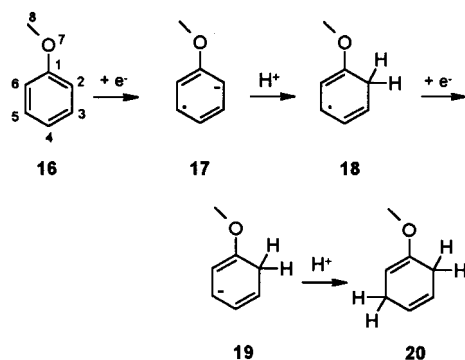
(15) (a) Zimmerman, H. E.; Wang, P. A. *J. Am. Chem. Soc.* **1993**, *115*, 2205–2216. (b) Zimmerman, H. E.; Wang, P. A. *J. Am. Chem. Soc.* **1990**, *112*, 1280–1281. (c) Birch, A. J. *Tetrahedron* **1959**, 148–153.

**Table 9.** Role of Electronegativity and Polarizability of the Nucleophile<sup>a</sup>

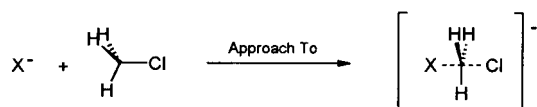
dist, Å	$\Delta D$ bond orders for the departing chloride				$\Delta D$ charge on the departing chloride			
	fluoride	chloride	bromide	iodide	fluoride	chloride	bromide	iodide
3.0 <sup>b</sup>	-15	-92	-116	-135	184	286	320	330
2.5	-74	-290	-367	-479	500	734	833	870
2.3	-131	-443	-564	-756	696	1018	1175	1254

<sup>a</sup> Use of 3.5 Å as a starting point. B3LYP/3-21G\*. <sup>b</sup> Distance between the nucleophile and the carbon.

**Scheme 8.** Birch Reduction Mechanism: The Anisole Example



**Scheme 9.** S<sub>N</sub>2 Reaction of Methyl Chloride and Halide Anion



question of which carbon of the radical anion is most electron-rich and protonated in the rate-limiting step. In the case of anisole we see from Table 8 that it is the ortho and meta positions which are most enhanced in density by electron introduction. The para site is not appreciably affected. Of course, the change in density, although of intrinsic interest, is not what is controlling but, instead, the total density at each site. Thus, the early reasoning that the introduced electron will avoid the ortho and para position is not logical.<sup>15c</sup> The initial ortho density in anisole is sufficiently higher than meta that with the increases, it is the ortho site which is most electron rich and hence protonated. The total radical-anion densities and the increases are given in Table 8.

The  $\Delta D$  approach was also applied to S<sub>N</sub>2 reaction of methyl chloride and halide anion (Scheme 9). The first ( $D^a$ ) matrix was obtained from an early complex (C...Cl<sup>-</sup> distance = 3.5 Å) and compared with the  $D^b$  matrices obtained from the single

point computations on a number of further steps along the S<sub>N</sub>2 reaction path with gradual decrease of the C-Halogen distance.

Two of the  $\Delta D$  elements were monitored. The first element corresponded to the change in the bond order of the breaking C-Cl bond, and the other element was the electron density on the departing Cl atom. Using these elements one can monitor the extent of electron transfer and concertedness of the bond forming/bond breaking processes. Table 9 illustrates the extent of these processes changing in the F-Cl-Br-I order. Here we see the increase in electron transfer (i.e. polarizability) in the sequence F < Cl < Br < I.

**Conclusion**

In this research we have used the Delta Density treatment to provide a comparison of molecular structures differing in geometry as well as in number of electrons. Hitherto, the method had been limited to a comparison of electronically excited species with their ground state counterparts. The present method extends the treatment to comparison of the corresponding basis set orbitals of any two corresponding species of interest. The power of the method is its ability to predict which bonds are most subject to being severed and which bonds are likely to be formed. In addition the method permits one to monitor the flow of electron density as reactions proceed. Hence the Delta Density method provides a quantitative counterpart of "electron pushing". Even to the extent that the results could be intuitively predicted by an experienced organic chemist, the agreement of the present theory with intuition is, in itself, both remarkable and of consequence. Indeed, hitherto, there has been a paucity of theory able to emulate the organic chemist's intuition.

**Acknowledgment.** Support of this research by the National Science Foundation is gratefully acknowledged with special appreciation for its support of basic research.

**Supporting Information Available:** Additional computational details (PDF). This material is available free of charge via the Internet at <http://pubs.acs.org>.

JA002402C